Received 28 February 2026
Revised 7 April 2026
Accepted 30 April 2026

Wear of contact strip in high-speed trains: a review

Dong Doan Van
Institution of Mechanical Engineers, Ho Chi Minh City University of Transport, Ho Chi Minh City, Vietnam and
BRIDGE Research Group, Ho Chi Minh City University of Transport, Ho Chi Minh City, Vietnam, and
Hue Phuoc Lu
BRIDGE Research Group, Ho Chi Minh City University of Transport, Ho Chi Minh City, Vietnam

Abstract

Purpose – The pantograph–catenary system (PCS) plays a crucial role in ensuring stable and continuous current collection in electric railway operations. This paper aims to review and synthesize existing research on contact strip (CS) wear, with particular emphasis on dominant wear mechanisms, influencing parameters, and material performance under high-speed train (HST) conditions.

Design/methodology/approach – A structured and critical review of the literature is conducted, covering mechanical, electrical, and electro-mechanical wear mechanisms. Relevant studies are analysed in terms of operating conditions, including train speed, contact force, electrical current intensity, system configuration and environmental influences. Special attention is given to metal-impregnated carbon materials, which are widely adopted in current HST applications, as well as to composite materials that are being actively investigated and developed for future HST systems. Comparative analysis is performed to identify governing factors and methodological trends in existing investigations.

Findings – The literature indicates that CS degradation results from strongly coupled mechanical and electrical loading, with the relative contribution of each wear mechanism varying according to operating regimes and material characteristics. Carbon-based composite materials demonstrate a favourable balance between conductivity, wear resistance and compatibility with the contact line (CL). However, inconsistencies remain in the quantification of wear interactions and in the standardisation of evaluation approaches under diverse climatic and operational conditions.

Originality/value – This review provides an integrated and up-to-date synthesis of multi-mechanism wear behaviour in CS, highlighting current research gaps and methodological limitations. The paper offers structured insight to support material selection, performance optimisation and future research directions, contributing to enhanced reliability and maintenance efficiency of HST systems.

Keywords Carbon-based composites, Contact strip, Current collection, High-speed trains, Wear behaviour

Paper type General review

1. Introduction

Along with societal development and the global trend of urbanization, high-speed trains (HST) have been increasingly regarded as a strategic solution to modern mobility demands, owing to their ability to simultaneously deliver high operating speeds, a high level of operational safety, and sustainability in urban development (Abd Majid & Mohd Zaki, 2025; Permalu & Nagarajoo, 2024). The rapid advancement of electric railway systems is widely considered to represent a significant transformation within the transportation sector, reflecting a broader shift toward smart urban mobility and sustainable transport development (Yang *et al.*, 2022; Zhao *et al.*, 2025).

The pantograph–catenary system (PCS) plays a pivotal role in the overall configuration of HST, directly determining operational safety and reliability. A schematic overview of the electrical system is presented in Figure 1. Electrical power for traction is supplied through the

Railway Sciences
Vol. 5 No. 4, 2026
pp. 524-547
Emerald Publishing Limited
e-ISSN: 2755-0915
p-ISSN: 2755-0907
DOI 10.1108/RS-02-2026-0014

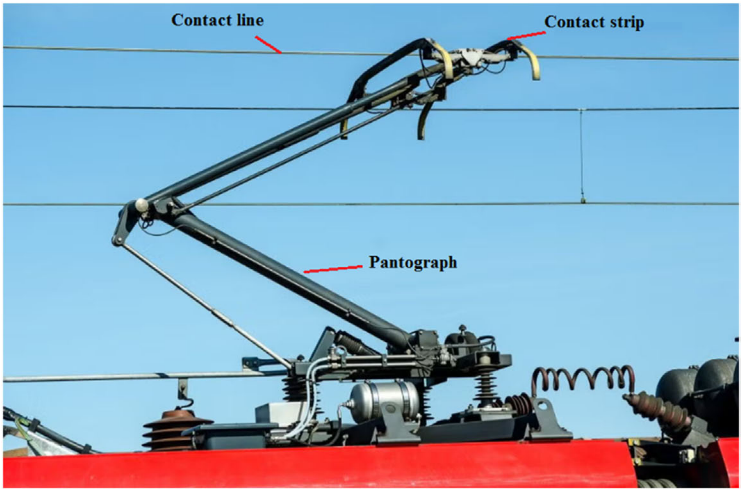

Figure 1. Electrical system schematic of a HST. **Source(s):** Nilson (2023)

overhead contact line (CL), which provides the energy required for HST operation. The pantograph, mounted on the roof of the train, serves as the device responsible for collecting electrical energy from the overhead contact system. The contact strip (CS), acting as the conductive component in direct contact with the CL, forms a sliding current collection interface (Wu *et al.*, 2022a). This system enables the transmission of electrical energy from traction substations to the train during motion. As a critical subsystem of electric traction systems for HST, the pantograph plays a key role in ensuring efficient and reliable power transmission. The operational performance of the pantograph has a significant influence on overall system efficiency and the development of electrified railway technologies (Liu *et al.*, 2020; Liu, Zhang, Li, Zhao, & Zhou, 2026). The primary technical characteristics of the pantograph, including material density, electrical conductivity, and impact resistance, are required to satisfy stringent standards to ensure stable operation and optimal performance (Bruni, Bucca, Facchinetti, Gregori, & Pombo, 2025; Jia, Li, Guo, Su, & Song, 2023).

The CS is a critical component of electric traction systems, directly influencing the efficiency and stability of current collection. The quality of the CS governs the reliability of electrical energy transfer between the pantograph and the CL. During operation, the CS is exposed to the ambient environment and subjected to combined mechanical, electrical, and aerodynamic loads, making it particularly susceptible to wear over extended service periods. As train operating speeds increase, the dynamic loads acting on the current collection system intensify, leading to more complex wear mechanisms and adversely affecting the reliability and service life of electrified railway systems (Xu *et al.*, 2024). Furthermore, the contact pressure between the CS and the CL is a key operational parameter that directly affects the reliability and durability of the current collection system. Excessive contact pressure can result in abnormal wear of both the CS and the CL, significantly shortening their service life. Conversely, insufficient contact pressure may cause interruptions in current transmission, leading to electrical arcing at the contact interface, which can damage or even burn the CL (Derosa, Nåvik, Collina, Bucca, & Rønnquist, 2021; Song, Mei, Liu, & Gao, 2023).

Abnormal wear of the CS is known to have a significant impact on train maintenance and operational performance. When the degree of wear exceeds allowable limits, the CS must be replaced more frequently to ensure continuity and safety during operation. However, such frequent replacements substantially increase maintenance costs and result in extended train downtime. In certain cases, if severe wear of the CS occurs while the train is in service, the monitoring system may automatically trigger the lowering of the pantograph in order to prevent equipment damage or electrical arcing. Such incidents not only disrupt train punctuality but also pose potential risks to the operational safety of the entire electric railway system (Zhi *et al.*, 2026).

Therefore, the accurate identification of the underlying causes of abnormal wear of the CS is of critical importance for ensuring operational safety and extending the service life of onboard electrical equipment. In this paper, the principal factors leading to CS wear are systematically analysed, and existing studies related to the early detection of damage and degradation of this component are comprehensively reviewed and evaluated. In addition, current research directions concerning materials used for CS are surveyed, with particular emphasis placed on emerging material development trends aimed at achieving enhanced wear resistance and improved electrical stability. The findings presented in this study are expected to provide a solid scientific basis for investigating wear mechanisms and for proposing effective technical measures to mitigate CS degradation. Consequently, the reliability and operational efficiency of the PCS in HST can be further improved.

The remainder of this paper is structured as follows. Section 2 describes the material structure of CS, focusing on their compositional design and functional requirements under high-speed current collection conditions. Section 3 analyses the principal mechanisms leading to CS wear, including mechanical wear, electrical wear, and electro-mechanical wear. Section 4 reviews current methods for the inspection and detection of CS abnormalities, covering both conventional diagnostic techniques and emerging monitoring technologies. Section 5 discusses open technical challenges and outlines prospective research directions aimed at improving durability, reliability, and predictive maintenance strategies. Finally, Section 6 concludes the paper by summarising the main findings and highlighting key implications for future developments.

2. Material structure of CS

The material of the CS plays a decisive role in the current collection quality of the electrical system. As the CS is in direct contact with the surrounding environment, it is subjected to various influences, including friction, temperature fluctuations, humidity, contamination by dust and debris, and electrical arcing. Consequently, the design of CS materials is required to simultaneously satisfy multiple performance criteria, including high wear resistance, corrosion resistance, high electrical conductivity, thermal stability, self-lubricating capability, and good impact resistance (Fadzil, Hyie, & Selamat, 2023). These key material characteristics are illustrated in Figure 2.

First, wear resistance is regarded as a critical requirement, as the CS is continuously subjected to friction against the CL under high contact forces and high operating speeds. The material is therefore required to maintain sufficient mechanical strength and a stable surface structure in order to limit material loss and extend service life. In addition, corrosion resistance is essential for suppressing chemical reactions induced by moisture, salt, air pollutants, and oxidation products generated during electrical arcing. High electrical conductivity is a mandatory property, as it reduces resistive losses, limits localized heat generation at the contact interface, and ensures efficient energy transmission. The CS material is also required to exhibit good thermal stability, particularly under severe operating conditions where surface temperatures may rise sharply due to high electrical currents or arc discharges. Self-lubricating capability represents another important material characteristic, as it contributes to lowering the friction coefficient, slowing wear progression, and mitigating stick–slip phenomena, thereby improving contact stability. Finally, adequate impact resistance and resistance to cracking are necessary to prevent material failure under strong vibrations, aerodynamic loads, or when encountering irregularities along the CL.

Research on CS materials has attracted considerable attention from the scientific community. At present, the materials commonly employed for CS can be broadly classified into five main categories: pure metal contact strips, pure carbon contact strips, powder metallurgy contact strips, metal-impregnated carbon contact strips, and composite contact strips (Wu *et al.*, 2022a; Zuo *et al.*, 2021a). The characteristic features of each material category are summarised in Table 1.

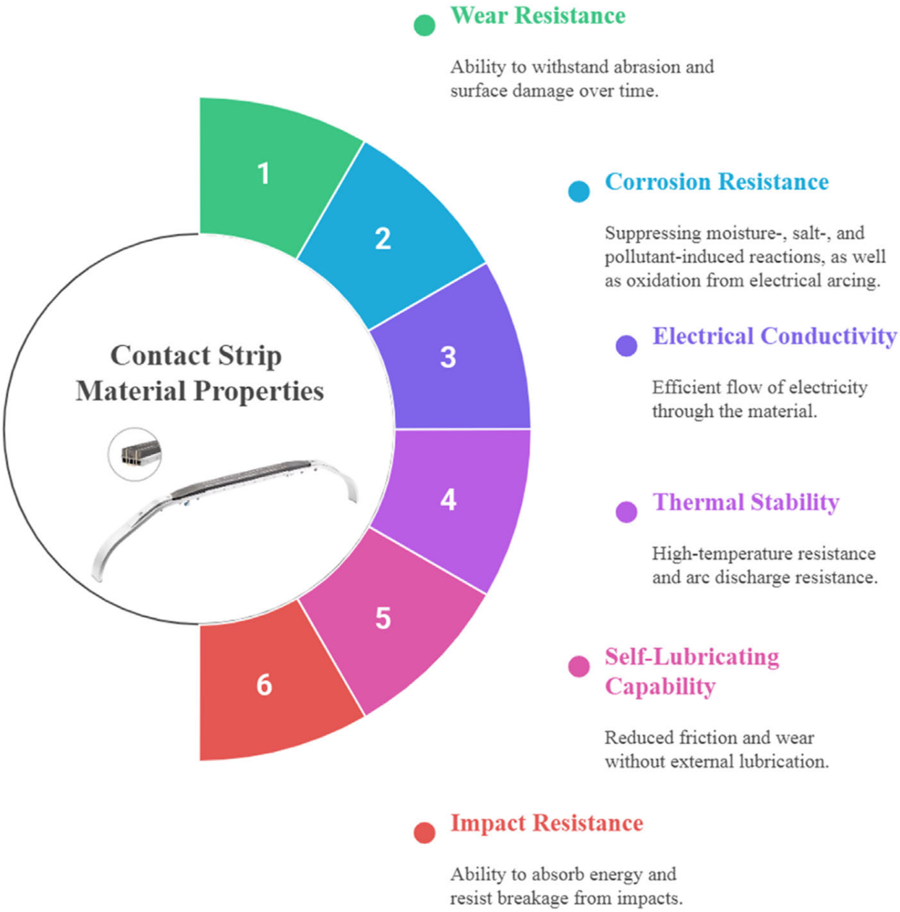

Figure 2. Material requirements for CS. **Source(s):** Authors’ own work

As shown in Table 1, the advantages and limitations of each material indicate that pure metal, pure carbon, and powder metallurgy CS are generally suitable only for low- and medium-speed train applications (≤200 km/h). Consequently, in order to meet the operational requirements of HST (>200 km/h) and future very-high-speed train systems, material research should be primarily focused on metal-impregnated carbon contact strips and composite materials. These material systems are expected to offer more comprehensive and superior performance in terms of wear resistance, electrical stability, and overall service reliability.

2.1 Metal-impregnated carbon contact strip

Metal-impregnated carbon contact strip are typically manufactured using a carbon/graphite matrix, which is subsequently infiltrated with metals such as copper, antimony, or silver in order to enhance mechanical strength, improve thermal conductivity, and reduce material porosity. Common techniques employed for producing metal-impregnated carbon/graphite materials include liquid metal infiltration and sintering processes combined with metal impregnation (Cantürk & Kováčik, 2022). The manufacturing process of the metal-impregnated carbon contact strip is illustrated in Figure 3, with the red line indicating the process flow.

Table 1. Classification and characteristics of CS materials

Type of CS	Advantages	Disadvantages
Pure metal contact strip	Low cost; high electrical conductivity; large current-carrying capacity; long service life; high mechanical strength	Poor self-lubricating ability; causes severe wear of the CL; limited resistance to high temperatures; prone to adhesion; susceptible to melting
Pure carbon contact strip	Good self-lubricating properties; significant friction reduction; good high-temperature resistance; adequate electrical conductivity; minimal damage to the CL; low mass	Low mechanical strength; prone to cracking or chipping under strong impacts; high wear rate; limited current-carrying capacity
Powder metallurgy contact strip	High mechanical strength; good wear resistance; good electrical conductivity; good impact resistance; moderate surface hardness	Poor self-lubricating performance; severe wear of the CL; limited resistance to electrical arcing
Metal-impregnated carbon contact strip	Good electrical conductivity; high thermal stability; good wear resistance; high mechanical strength; low contact resistance with the CL; long service life; good resistance to arc erosion	High maintenance cost; poor impact resistance; prone to cracking or chipping
Composite contact strip	High mechanical strength; low weight; good resistance to electrical arcing; good wear resistance; good thermal stability; excellent impact resistance and self-lubricating properties	High cost; long manufacturing cycle; potential degradation of electrical conductivity; limited high-temperature resistance; susceptibility to thermal decomposition

Source(s): Authors' own work

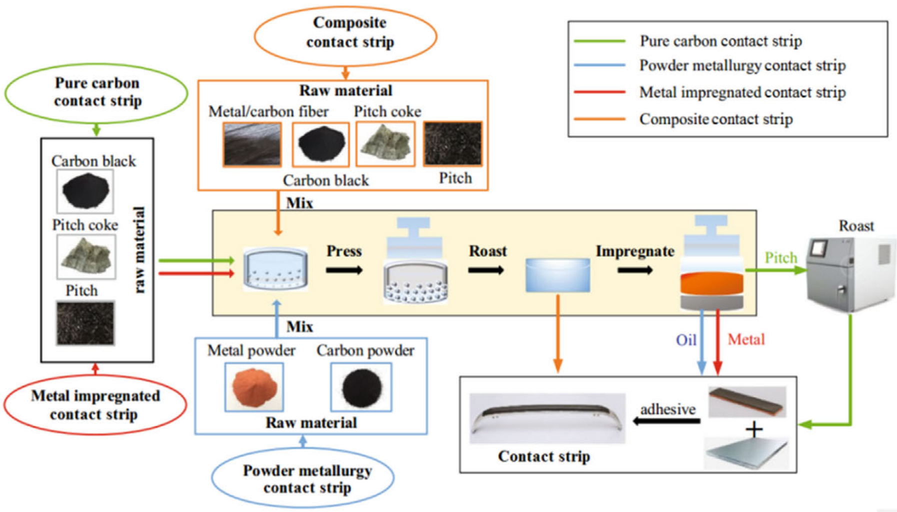

Figure 3. Schematic of the CS manufacturing process. **Source(s):** Wu *et al.* (2022a)

Metal-impregnated carbon contact strip are commonly fabricated using melt infiltration techniques, which are carried out in sealed chambers under controlled pressure conditions and at elevated temperatures. Typical melt infiltration methods include vacuum infiltration, pressureless infiltration, and pressure-assisted infiltration (Biswas *et al.*, 2024; Ma *et al.*, 2020). These processes indicate that melt infiltration is a key factor governing the interfacial bonding strength between the carbon matrix and the infiltrated metal. The effectiveness of melt infiltration is generally quantified by the contact angle: a contact angle greater than 90° indicates poor wettability, whereas a contact angle less than 90° corresponds to good wettability between the carbon substrate and the molten metal (Cantürk & Kováčik, 2022).

Kong, Ru, Zhang, and Fan (2018) reported that a Cr_3C_2 coating was applied to copper-infiltrated carbon–carbon (C/C) composites. The results demonstrated that the wettability between the carbon surface and molten copper was significantly improved, with the contact angle reduced from 140° to 60°. In addition, the resulting C/C composite exhibited a porosity of 4.2% and a density of 3.69 g/cm^3, together with enhanced electrical and thermal conductivity. Both compressive and flexural strengths were markedly improved, while a low friction coefficient and reduced wear rate were achieved. These results confirm the strong potential of C/C–Cu composites for practical application as current-collecting materials for pantographs. Zuo *et al.* (2021b) investigated carbon-copper (C/Cu) and Cu–B/carbon materials sintered from copper–boron alloys using melt infiltration techniques. The results indicated that the contact angle was reduced from 123.6° to 21.3°, demonstrating a significant improvement in wettability. Furthermore, the compressive and flexural strengths were increased by 39% and 54%, respectively. The minimum electrical resistivity of 1.7 μΩ·m was achieved at a boron content of 1.2 wt%, highlighting the effectiveness of boron addition in enhancing both mechanical and electrical performance. Zhang, Guo, Zhao, Zhang, and He (2020) examined the interfacial microstructure formed during the melt infiltration of C/C materials with Cu–8 wt% Ti at 1373 K for 30 minutes was examined. The results revealed the formation of two distinct interfacial contact regions: one consisting of a copper layer with a maximum thickness of approximately 500 nm at the interface between pyrolytic carbon (PyC) and coarse-grained TiC (CG), and another comprising fine-grained TiC (FG) mixed with nanoscale copper particles. Zuo *et al.* (2021c) investigated reaction products formed between iron (Fe) and C/Cu materials were investigated. The Fe element was found to be distributed between the carbon matrix and the copper phase, with carbon reacting to form an Fe_3C interfacial layer. The results indicated that the contact angle was reduced from 124° to 21°, demonstrating significantly improved wettability. However, the electrical resistivity was increased by approximately six times compared with that of the material without Fe addition.

At present, many countries worldwide have developed and manufactured metal-impregnated carbon CS with technical characteristics tailored to the requirements of their respective electric train systems. Table 2 presents representative characteristic parameters of CS employed in several typical countries.

2.2 Composite contact strip

Compared with metal-impregnated carbon contact strips, composite contact strip exhibit superior mechanical strength and enhanced wear resistance. Composite contact strips are defined as multi-phase engineered materials consisting of a carbon-based matrix combined with reinforcing or functional constituents including carbon fibers, metal fibers, metallic phases, ceramic particles (e.g., carbides), or hybrid architectures and are fabricated through specialized mixing and processing techniques to achieve a synergistic combination of properties. Figure 3 illustrates the manufacturing process of the composite contact strip, where the orange line denotes the process flow.

For metal-carbon fiber–reinforced composite CS, chemical surface treatment is required to enhance fiber surface stability and to prevent carbonization. Lee, Kim, Kim, and Kim (2023) demonstrated that optimized silane treatment of recycled carbon fibers significantly increased interfacial shear strength and the oxygen content on the fiber surface, indicating enhanced surface activity and improved interfacial bonding. These findings can be directly applied to the development and performance improvement of composite CS. Wang *et al.* (2020) demonstrated that a TiO_2 coating formed on a carbon substrate via the sol–gel method

Table 2. Specifications of metal-impregnated carbon CS in selected countries

Manufacturer	Description	Density (g/cm^3)	Electrical resistivity (μΩ·m)	Flexural strength (MPa)	Source
Mersen (P5696)	Metal impregnated (22% Cu)	2.25	6	70	Mersen (2024)
Mersen (P2805)	Metal impregnated (28% Cu)	2.4	3.5	70	Mersen (2024)
Mersen (P3210)	Metal impregnated (32% Cu)	2.5	2.2	85	Mersen (2024)
Morgan (MY131)	Metalised carbon light weight lead free	2.2	8	60	Morgan (2024)
Morgan (MY7A2)	Metalised carbon low resistivity for general applications lead free	2.4	4	60	Morgan (2024)
Morgan (MT85A)	Metalised carbon low resistivity for general applications lead free	2.4	3	65	Morgan (2024)
Morgan (MY258A2)	Metalised carbon low resistivity for high current applications lead free	2.7	2	60	Morgan (2024)
Morgan (MY258A4)	Metalised carbon low resistivity for high current applications lead free	2.8	1	60	Morgan (2024)
Pantrac (RH83M6)	Impregnated carbon	3.4	7	102	Pantrac (2024)
Elekro Karbon a.s. (SK162)	Metal impregnated (Cu)	2.3	5	60	Fadzil *et al.* (2023)
L. T graphite (PCS-30)	Metal impregnated (32% Cu)	2.5	2.2	80	L. T graphite (2024)
Morteng (CK20)	higher strength and lower resistivity	2.7	5	75	Morteng (2024)
Morteng (CK50)	carbon based material-impregnated material, good conductivity, strength, and density	2.3	5	85	Morteng (2024)
Morteng (CK80)	Carbon based metal impregnated material, less copper infiltration, relatively light	2	8	80	Morteng (2024)

Source(s): Authors' own work

produced a uniform and chemically stable layer, which enhanced surface protection and effectively maintained structural integrity. Tian *et al.* (2026) applied a specially formulated phosphate conversion coating to the surface and observed a significant reduction in surface degradation under corrosive and wear conditions. These results indicate the strong potential of chemical surface treatment methods for enhancing the durability and stability of fibers in metal-carbon fiber–reinforced composites, which can be directly applied to CS.

Carbon/carbon composite CS consist of carbon fibers reinforced within a carbon matrix and are distinguished by their excellent high-temperature resistance and thermo-mechanical stability at high operating speeds, making them particularly suitable for pantograph contact systems of HST. At present, such materials are mainly fabricated using two principal approaches.

The first approach employs a hybrid reinforcement of continuous long carbon fibers and chopped carbon fibers to optimize both mechanical performance and electrical conductivity. The fibers are blended according to a designed ratio and subsequently consolidated by hot pressing or cold pressing to form a green preform, followed by successive cycles of resin impregnation, carbonization, and graphitization to achieve the required strength and density. This method enables improved control over matrix structure and facilitates the formation of a continuous conductive network within the composite.

The second approach is based on continuous carbon fibers in the form of woven fabrics. In this case, carbon fiber fabrics are tailored with optimized fiber orientations for load-bearing capacity and electrical conduction, impregnated with resin or pitch/phenolic binders, and then subjected to multiple impregnation, carbonization, densification, and graphitization cycles to increase density, enhance mechanical strength, and improve resistance to electrical arcing (Agarwal *et al.*, 2024; Jiang *et al.*, 2025).

Surface treatment of carbon fibers is essential in carbon/carbon CS to improve interfacial adhesion between the fibers and the matrix, enhance metal impregnation (e.g., copper), and ensure stability under thermal loading, wear, and electrical arcing conditions. The pristine surface of carbon fibers is typically chemically inert and contains a limited number of active functional groups, resulting in poor wettability with resins or metals and weak fiber–matrix bonding. This deficiency can lead to degraded mechanical performance and reduced service life of the composite material (Peng, Wu, & Wei, 2024). Through treatments such as acid oxidation, plasma treatment, or chemical coating, polar functional groups (e.g., –COOH, –C=O) are introduced onto the fiber surface, while surface roughness is simultaneously increased. These modifications improve wettability, raise surface energy, and consequently enhance fiber–matrix interfacial bonding (Ansari, Zafar, & Pathak, 2023). Furthermore, in C/C–Cu (carbon/carbon copper-impregnated) designs, surface-treated fibers promote more effective copper infiltration into the fiber structure, reduce defects, facilitate the formation of a continuous electrical conduction network, and suppress arc-induced wear. As a result, the overall performance and durability of CS are significantly improved.

Wang *et al.* (2023a) evaluated the performance of C/C–Cu and C/C–Cuf composite contact strip in comparison with pure carbon contact strips, with the aim of enhancing electrical conductivity, mechanical properties, and wear resistance under current-carrying conditions. The results showed that the C/C–Cu contact strips exhibited a significantly lower friction coefficient, reduced wear rate, and markedly lower arc energy than both pure carbon and C/C–Cuf contact strips. Wear surface analyses revealed that C/C–Cu was capable of forming a stable crystalline layer, which acted as a self-generated solid lubricating film and effectively improved friction and wear behavior. Overall, the study demonstrated that copper incorporation into the C/C matrix represents an effective strategy for upgrading CS, particularly for applications involving high electrical currents and demanding contact durability requirements. Li *et al.* (2022) developed a carbon/needle-coke composite reinforced with copper fibers (CF NC/C) for CS applications, aiming to enhance electrical conductivity, mechanical performance, and wear resistance under current-carrying conditions. The results indicated that the CF NC/C sample containing 5 wt% copper fibers achieved a density of 1.8788 g/cm^3, an electrical resistivity of 35.18 $\mu\Omega \cdot$m, and an impact strength of 0.16 J/cm^2. In addition, this composition exhibited the lowest friction coefficient and the smallest wear rate among the tested specimens under electrical loading. The uniform distribution of copper fibers achieved through the rolling process contributed to maintaining a stable carbon matrix structure, while the incorporation of needle coke further improved mechanical properties and current-carrying capability.

Wang *et al.* (2021) reported a novel CS fabricated from a carbon-fiber-reinforced polymer (CFRP) composite and further integrated with a copper mesh. The manufacturing process involved impregnation with a resin containing carbon fibers and flake graphite, followed by hot molding. The results demonstrated that the composite exhibited significantly lower electrical resistivity compared with pure carbon contact strips. The addition of carbon fibers markedly improved impact strength and wear resistance. Furthermore, both electrical resistivity and the friction coefficient decreased as the graphite content was increased from 0 to 15 wt%.

Recent developments have introduced advanced composite systems such as multi-carbide composites (MCC), in which multiple carbide phases (e.g., SiC, TiC) are incorporated into a carbon matrix (Wu *et al.*, 2022a). These materials, particularly those based on MAX phase ceramics (Atazadeh, Heydari, Baharvandi, & Ehsani, 2016), exhibit significantly enhanced electrical conductivity, mechanical strength, oxidation resistance, and thermal stability compared to conventional carbon-based strips. Similarly, carbide-reinforced composites such as C/C–SiC systems have demonstrated improved hardness and tribological performance due to reduced chemical reactivity and enhanced structural stability (Kumar & Srivastava, 2016).

In addition to the aforementioned composite pantograph contact strips, recent studies have increasingly focused on multi-phase composite systems for pantograph applications. These materials consist of a carbon-based matrix integrated with multiple reinforcing and functional phases, including metals, ceramic particles, and fibers (Tan *et al.*, 2022; Wang *et al.*, 2020). Wang *et al.* (2022b) investigated Al_2O_3–ZrO_2–C multi-phase composites incorporating nano-oxide additives (nano-ZrO_2, nano-TiO_2, and nano-Al_2O_3). Their results showed that these nano-phases promote the in-situ formation and growth of SiC nanowires, leading to an increased aspect ratio and improved microstructural connectivity. Consequently, the composites exhibited enhanced sinterability, thermal shock resistance, and oxidation resistance. These findings highlight the critical role of nano-scale additives and phase interactions in tailoring the microstructure and performance of multi-phase composite systems. Ban *et al.* (2020) investigated the incorporation of ZrB_2–SiCw composite powders into Al_2O_3–ZrO_2–C multi-phase CS materials to enhance corrosion resistance. Their results indicated that the introduction of ZrB_2 and SiC whiskers significantly improved the microstructural integrity by promoting a more compact and interconnected phase distribution. In addition, the presence of SiCw contributed to crack deflection and bridging mechanisms, while ZrB_2 enhanced resistance to slag corrosion and high-temperature degradation. As a result, the modified composites exhibited improved corrosion resistance and overall durability, demonstrating the effectiveness of multi-phase reinforcement strategies in optimizing CS performance under harsh operating conditions.

3. Causes of CS wear

3.1 Wear mechanisms

During HST operation, the CS comes into direct contact with the overhead CL to collect electrical current for the train's power system. While in motion, relative sliding occurs continuously between the CS surface and the CL under high contact pressure, generating friction and wear (Du *et al.*, 2025). CS wear can be classified into three main categories depending on the dominant influencing factors: mechanical wear, electrical wear, and electro-mechanical wear. The wear rate of the CS is directly affected by the temperature generated at the contact interface, which primarily arises from mechanical friction, contact resistance, and electrical arcing during current collection (Ren & Chen, 2023; Zhou *et al.*, 2024b).

3.2 Mechanical wear

Mechanical wear occurs due to the continuous sliding friction between the CS and the CL. The contact force exerted by the pantograph (70–120 N), combined with the high train speed (>350 km/h), generates substantial contact pressure. When coupled with environmental influences, this leads to material detachment and loss from the CS surface (Haeg, 2025). According to Archard (1953), the volume of material removed by wear is proportional to the applied normal load and the sliding distance, and inversely proportional to the hardness of the softer material (Wang, Wang, Ge, Si, & Yang, 2023b), which can be expressed as follows:

$$V = k\frac{F.s}{H} \tag{1}$$

Where: V is the volume of material worn; k is the wear coefficient; F is the contact force; s is the sliding distance; and H is the material hardness.

Mechanical wear of CS primarily includes adhesive wear, abrasive wear, and fatigue wear. These mechanisms can occur sequentially or simultaneously, interacting with one another to produce surface degradation.

Adhesive wear arises when two contacting surfaces are subjected to high contact pressure. At microscopic asperities, friction generates localized high temperatures, causing the contact points to adhere. During relative motion between the surfaces, these adhered points are sheared off, resulting in the detachment of material fragments. This process transfers material from one surface to the other or produces loose wear debris (Zhang, Goltsberg, & Etsion, 2022).

Abrasive wear occurs when hard particles or contaminants such as dust, metal oxides, or sand grains enter the contact zone between the CS and the CL, or when surface asperities interact during sliding. These particles act as micro-cutting tools, producing scratches and material removal on the surface (Derosa, Nåvik, Collina, Bucca, & Rønnquist, 2020), as illustrated in Figure 4a. This mechanism can be classified into two types: two-body wear, where the CS and CL directly abrade each other, and three-body wear, where intermediary particles move between the two surfaces and induce wear. The characteristic surface morphology of abrasive wear consists of grooves aligned parallel to the sliding direction. The wear rate increases significantly when trains operate in dusty or desert environments. Consequences of abrasive wear include reduced surface flatness, increased pantograph oscillation, and conditions favorable to electrical arcing, which can subsequently lead to electrical wear.

Fatigue wear occurs when the CS surface is subjected to repeated stresses caused by continuous pantograph oscillations following the CL profile. This process leads to the initiation of microcracks, and over time, thin layers of material peel off in flakes, resulting in reduced surface durability. The characteristic features of fatigue wear include pitting or the delamination of thin carbon layers on the CS surface. This mechanism is closely related to the oscillation frequency of the pantograph, the surface roughness of the CL, and is strongly promoted under high train speeds or large oscillation amplitudes. In addition, irregularities in the pantograph suspension system or uneven catenary sag increase repeated stresses, thereby accelerating fatigue wear (Zhi *et al.*, 2026).

3.3 Electrical wear

Electrical wear occurs when oscillations at the contact interface cause intermittent current flow, leading to the formation of electrical arcs. Temperatures in the arc region can reach 2000–4,000 °C, causing localized melting and vaporization of material on the contact surface. Common types of electrical wear include arc erosion, in which material melts and vaporizes, producing a roughened surface, and melting wear, which results in burnt areas, flowing

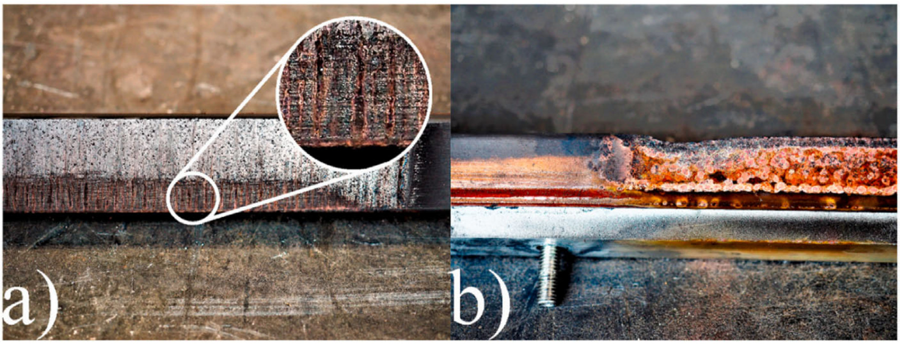

Figure 4. Wear of CS: (a) mechanical wear; (b) arc erosion wear. **Source(s):** Derosa *et al.* (2020)

material, or small craters on the surface. Manifestations of electrical wear include blackened scorch marks, small pits, or thermal cracks. This mechanism is particularly pronounced when the CL is uneven, the pantograph undergoes large oscillations, or the electrical contact quality is poor (Hu, Huang, Cheng, Zhang, & Ma, 2024), as illustrated in Figure 4b.

On the surface of the CS, the effective heat flux responsible for heating and splashing molten material is defined as follows (Tian, Wang, Lu, & Li, 2025):

$$q_a = h_a(T - T_0) \tag{2}$$

Where: q_a is the effective heat flux; h_a is the heat transfer coefficient associated with arc heating; T_0 is the local surface temperature of the material; T is the arc temperature.

When T_0 reaches a high temperature exceeding the critical temperature, the molten splashing process occurs; when T_0 is below the material's critical failure temperature, the effective heat flux is used to heat the material in its solid state. The molten splashing process can be described as follows:

$$v_a = \frac{q_a}{\rho H_s} \tag{3}$$

Where: ρ is the material density, and H_s is the boiling point of the material.

3.4 Electro-mechanical wear

The heat generated by friction between the CS and the CL is generally relatively small, whereas Joule heating can cause significant surface temperature variations. As the temperature rises, the surface material softens, and oxide layers as well as molten material layers form on the CS surface. Under repeated oscillatory stresses, the softened material begins to develop surface cracks. As the crack density increases, material gradually detaches and flakes off the surface (Dong, Li, Chen, Wang, & Zhang, 2025). Some of the detached material remains adhered within the friction pair, forming wear particles distributed in arc-induced pits and on the contact surface. This phenomenon increases surface roughness, leading to higher vibration and impact during contact. The combination of intense vibration and surface material loss causes arc-eroded regions to coalesce, forming extensive flaked areas (Song, Bi, & Wu, 2025). Under the influence of electrical current, the fatigue spalling rate of the surface material is further accelerated, while the number of arc-induced pits increases. The presence of wear particles exacerbates granular wear, and the elevated temperature promotes material oxidation, leading to more severe adhesive wear.

Therefore, it can be concluded that the electrical current primarily affects the CS surface by increasing the temperature, and electro-mechanical wear constitutes a characteristic wear mechanism that plays a crucial role in the degradation of CS performance.

3.5 Influence of the CL

The design and layout parameters of the overhead CL directly influence the wear characteristics of the CS during current collection. Tension, diameter, sag, and gradient are key factors that determine the quality of contact between the line and the CS.

Firstly, the tension of the CL affects the stability of the wire position during HST operation. Insufficient tension allows the wire to oscillate and sag significantly, requiring the pantograph to adjust continuously to maintain contact, which leads to fluctuations in contact force and intermittent current flow. These oscillations increase mechanical wear due to impact and electrical wear caused by arcing at the contact interface. Conversely, excessive tension raises the overall stiffness of the system, resulting in higher reactive forces at the contact point, stronger material detachment, and increased adhesive wear. In addition, the wire diameter plays a significant role: a larger diameter reduces current density and contact temperature, mitigating arcing; however, an excessively large diameter increases the wire mass and sag, inducing undesirable mechanical oscillations (Hayes, Fletcher, Beagles, & Chan, 2020; Sunar & Fletcher, 2023).

In addition to the factors above, the slope or lateral offset of the CL is an important design parameter for evenly distributing contact across the entire CS surface. In practice, the CL is not laid straight along the track direction but is intentionally offset alternately on either side of the pantograph center. This arrangement helps to disperse contact pressure and prevents localized wear at a fixed position on the CS. Simultaneously, as the contact point continuously shifts laterally, allowing previously loaded regions of the CS to dissipate heat and reduce thermal accumulation, thereby mitigating adhesive wear and material degradation. If the wire were laid straight, repeated pressure and heating at the same location would cause severe adhesive wear, forming deep grooves in the middle of the CS and significantly shortening its service life. However, excessive lateral offset or uneven placement between spans increases lateral pantograph oscillations, leading to higher vibrations and a greater risk of contact loss (Simarro, Postigo, Casanueva, Rodríguez-Tembleque, & Castillo, 2024).

3.6 Influence of the pantograph

The pantograph is a key intermediary component in the current collection system, responsible for maintaining stable electro-mechanical contact between the CS and the overhead CL to transmit electrical current to the train. The structural characteristics, contact force, and dynamic oscillations of the pantograph, together with external factors such as train speed, vibrations, and aerodynamic conditions, directly influence the extent and mechanisms of CS wear. Specifically, the contact force is a critical parameter for current transmission quality: if the force is too low, contact becomes unstable, leading to intermittent separation accompanied by arcing, which causes electro-mechanical wear due to localized heating and electrochemical corrosion; conversely, excessive contact force increases friction, resulting in mechanical wear, fatigue cracking, and surface deformation of the CS. The pantograph's dynamic oscillations, particularly at high speeds, cause significant variations in contact force, generating impacts and uneven wear. When the pantograph oscillation frequency resonates with the CL, impact forces are amplified, leading to increased impact wear and arc erosion (Amano, Kobayashi, Yabuno, Yamashita, & Mori, 2024; Santamato, Chiaradia, Solazzi, & Frisoli, 2023).

In addition, aerodynamic factors play a significant role: at high speeds, airflow disturbances around the pantograph head generating aerodynamic lift forces that modify the contact force and introduce significant force fluctuations, which may increase the frequency of contact loss and thereby promote arcing. Vibrations from the train carbody and suspension system also affect the dynamic stability of the pantograph; if the amplitude or frequency of these vibrations approaches the pantograph's natural frequency, resonance occurs, causing large fluctuations in contact force and severe impact wear. The mass and stiffness of the pantograph head suspension spring are also critical factors: an overly stiff system causes the pantograph to respond slowly to CL oscillations, resulting in strong impacts and localized wear, whereas an overly soft system can lead to intermittent contact and arcing (Wu, Gu, Ma, & Wang, 2022b).

Furthermore, the geometric design of the pantograph also affects wear distribution: the single-arm pantograph, with its lower mass and higher stiffness, helps reduce oscillations and maintain stable contact, whereas the double-arm pantograph is more prone to resonance with the CL, increasing localized wear, as illustrated in Figure 5. When the CS is not aligned parallel or perpendicular to the CL, uneven load distribution occurs, resulting in uneven surface wear or edge wear. In addition, high current through the pantograph alters the contact resistance, generating Joule heating and thermal fatigue, which further accelerates overall wear.

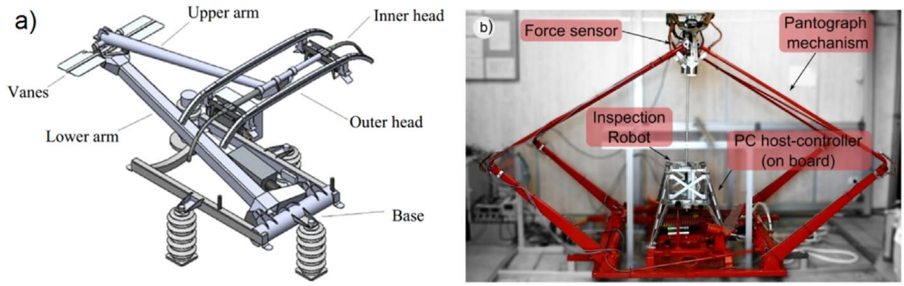

Figure 5. Pantograph configurations: (a) single-arm type; (b) double-arm type. **Source(s):** Wu *et al.* (2022a), Santamato *et al.* (2023)

3.7 Influence of environmental conditions

External environmental conditions play a crucial role in the wear mechanisms of CS, affecting them through various physical, chemical, and aerodynamic factors. Ambient temperature and humidity directly influence the contact surface: high temperatures soften the surface material, reducing mechanical strength and increasing both mechanical wear and deformation, while high humidity or condensation forms a thin water film, raising contact resistance, generating Joule heating and localized arcing, and promoting electro-mechanical wear. However, the influence of humidity is not entirely detrimental: a certain level of moisture may facilitate the formation of oxygen-rich tribofilms at the interface, which can reduce friction and mitigate wear under specific conditions. In ion-rich environments, such as coastal areas or polluted regions, electrochemical corrosion combined with mechanical friction and arcing leads to complex wear, accelerating CS degradation. Dust, debris, or ice accumulation on the CL increases surface roughness, creating stress concentration points and localized wear (Ning *et al.*, 2024; Zhi *et al.*, 2025, 2026).

Indeed, Yao, Zhou, Mei, and Zhang (2020) reported that as the thickness of the ice layer on the CL surface increases, the quality of current collection deteriorates significantly. Moreover, when train speed increases in the presence of ice accretion, the degradation in current collection performance becomes more severe. Under low-temperature operating conditions, it has also been observed that, in addition to the adverse effects on current collection quality, the hydraulic damper of the pantograph is substantially affected. Wang, Liang, Zhang, and Iwnicki (2019) reported that low temperatures increase the damping force, while the lowering efficiency of the pantograph is significantly reduced due to instability in the damping characteristics.

Furthermore, airflow around the pantograph particularly at high train speeds or under seasonal winds and turbulence causes fluctuations in contact force, leading to impacts and uneven wear. Thermal cycles, vibrations, and aerodynamic conditions also contribute to mechanical fatigue, microcracking, and alterations in contact geometry, creating conditions for concentrated wear (Daocharoenporn & Mongkolwongrojn, 2023).

Specifically, in Vietnam's tropical monsoon climate characterized by high humidity, frequent rainfall, and coastal salt exposure environmental factors further accelerate CS wear. A persistent moisture film on the CS and CL increases electrical resistance, generating localized heating and arcing. High temperatures, combined with friction and current flow, soften the material, promoting mechanical wear and surface deformation. Daily thermal cycles induce thermal fatigue and microcracks, which act as sites for concentrated wear (Zhi *et al.*, 2026).

It has been observed that high interface temperatures significantly affect the failure characteristics of the C–Cu contact interface during electrical sliding between contact pairs (Wang *et al.*, 2022a). When elevated temperatures occur, surface cracking is induced, and the rapid recovery contributes to an increased wear rate of the carbon material under high current conditions. It was demonstrated by Liu *et al.* (2021) that increasing temperature significantly affects frictional behavior, leading to a marked enhancement of adhesive wear and a concurrent exacerbation of oxidative wear.

Li, Zhao, Ji, Dong, and Wei (2025) investigated arc characteristics and erosion behavior of the frictional contact pair under varying humidity levels. The results indicate that the influence of humidity is non-monotonic. At moderate humidity, current transmission efficiency is improved and energy loss is minimized, leading to more stable electrical contact. However, as humidity further increases, the formation of a water–oxide film on the contact surface leads to higher average contact resistance and accumulated arc energy, thereby reducing electrical stability. Under high humidity conditions (e.g., 90% RH), white deposits were observed on the carbon surface, indicating the formation of oxide layers, as shown in Figure 6. The increase in humidity was found to promote the electrochemical oxidation of metals. The electrochemical reactions can be expressed as follows:

$$Cu + H_2O \rightarrow CuO + 2H^{+} + 2e^{-} \tag{4}$$

Under high humidity conditions, the coefficient of friction of current-carrying roller pairs was observed to increase, and the adhesion caused by electrical current, along with the surface friction induced by the current, was found to generate additional frictional forces. With the increase in friction coefficient, the wear mechanism of the current-carrying roller pairs was reported to transition from adhesive and sliding wear to fatigue wear (Song *et al.*, 2021; Wu *et al.*, 2022c).

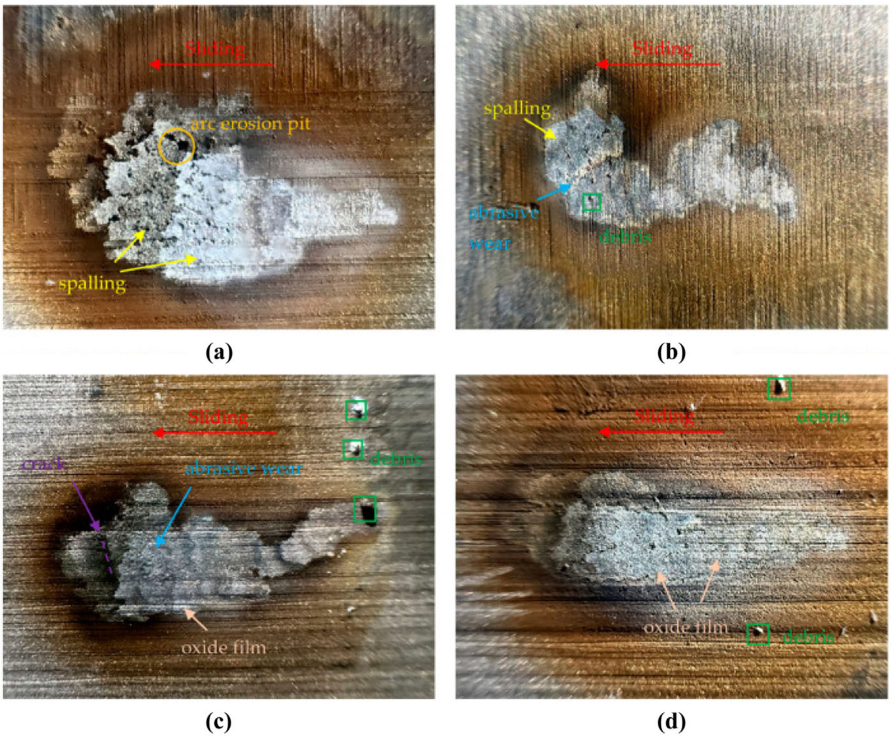

Figure 6. The surface morphology of the friction pair electrodes erosion under: (a) 30% RH; (b) 50% RH; (c) 70% RH; (d) 90% RH. **Source(s):** Li *et al.* (2025)

Additionally, monsoon winds and turbulent airflow cause fluctuations in pantograph contact force, increasing impact wear and uneven material loss. Low air pressure and strong airflow were identified as having a significant impact on pantograph contact performance. Xu *et al*. (2021) it was reported that when the PCS operated under low air pressure, the arc burning time and arc root quenching time were observed to increase substantially, resulting in more severe electrode wear. Air pressure was shown to have a significant effect on the oscillatory behavior of the arc column. Dong *et al.* (2023) it was observed that when the air pressure exceeded 2 kPa, the arc column exhibited substantial oscillations, with the lower part of the column oscillating less than the upper part. Conversely, when the air pressure was below 2 kPa, the arc was observed to be more stable.

In coastal regions, dissolved salts in water vapor and rain enhance electrochemical corrosion, further accelerating wear. When combined with moisture films, these ions facilitate the breakdown of passive oxide layers and accelerate electrochemical corrosion, significantly increasing the corrosion rate of metals exposed to marine atmospheres (Daneshian, Höche, Knudsen, & Skilbred, 2023). It has been reported by Liu, Mao, and Li (2025) that the performance of carbon contact strips under electrical contact conditions is affected by different salt spray exposures. The results indicated that increasing the salt spray concentration exacerbated pitting damage and increased surface roughness. The presence of elevated chloride concentrations and prolonged wetness enhances localized corrosive reactions, leading to more rapid material degradation under humid, salt-laden conditions.

Therefore, CS wear under Vietnam's environmental conditions occurs simultaneously through multiple mechanisms electro-mechanical, chemical, and nonlinear mechanical necessitating regular maintenance, the use of heat- and corrosion-resistant materials, and optimization of contact force and pantograph vibration to extend service life and enhance the reliability of the current collection system.

4. Methods for inspection and detection of CS abnormalities

Current methods for assessing CS wear are primarily based on direct measurement techniques. This procedure requires skilled technicians to accurately identify the extent of wear, as illustrated in Figure 7. After the train is brought into the depot and fully de-energized, personnel must climb onto the roof and use specialized measurement instruments to determine the CS thickness, locate worn areas, and evaluate material loss. While this approach is simple and straightforward to implement, it is relatively complex in practice due to the need for power shutdown and manual roof access. Furthermore, measurement results are highly influenced by human factors, introducing potential errors in identifying the most worn regions. In addition, this method only collects thickness values at discrete points, limiting the ability to accurately assess the overall wear morphology of the entire CS surface (Lu, Liu, Li, & Shen, 2021).

Figure 7. Technicians measuring wear on the CS. **Source(s):** Lu *et al.* (2021)

Currently, CS scanning devices have been developed to overcome the limitations of discrete measurement data. These devices allow direct acquisition of the three-dimensional geometry of the CS without requiring pre-defined reference points, enabling extraction of detailed surface structural parameters. Additionally, indirect detection systems using computer vision or laser technology can be installed at stations or along the track. As a train passes, these systems automatically capture the geometric features of the CS and employ image recognition and 3D reconstruction techniques to scan the surface, determine the minimum remaining thickness, and assess the wear characteristics, as illustrated in Figure 8 (Yao, Xing, Sheng, & Chen, 2022).

Yang *et al.* (2024b) proposed a high-accuracy 3D imaging method for CS was proposed. A color speckle pattern combined with an interferometric fringe sequence was projected onto the CS surface, and the reflected patterns were captured by two cameras, as illustrated in Figure 9. Experiments were conducted on a calibrated optical sphere, and a reconstruction error of approximately 0.07 mm in radius was observed, demonstrating that shallow defects with a size of about 1.0 mm could be detected and reconstructed. The reconstruction process was found to remain stable under varying illumination conditions, with a maximum error of 1.25 mm. Under optimal conditions, the mean reconstruction error was measured to be less than 0.25 mm, indicating that the method can reliably be applied for the inspection and condition assessment of CS in practical operations. Karaduman and Akin (2020) developed a convolutional neural network (CNN) architecture was developed to detect the wear level of CS. Images of the CS were collected from real operations and were preprocessed using a Power Law Transformation to enhance image quality prior to being input into the model.

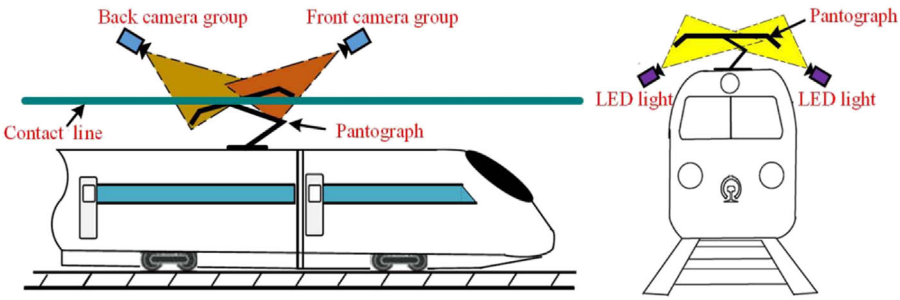

Figure 8. Automated device for detecting CS wear. **Source(s):** Yao *et al.* (2022)

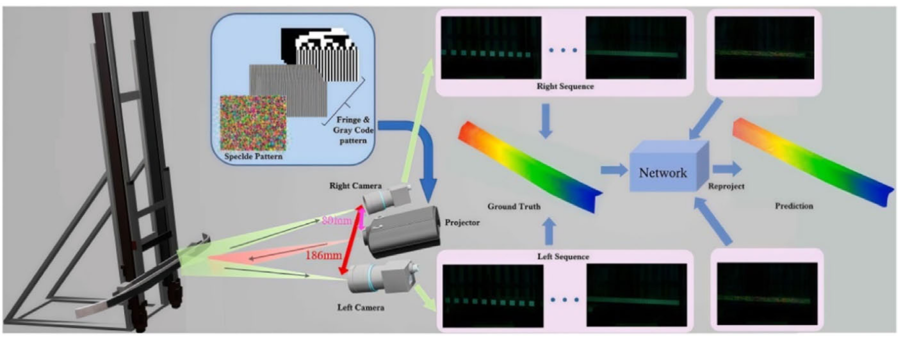

Figure 9. Setup of cameras and projector. **Source(s):** Yang *et al.* (2024b)

Subsequently, a Hough Transform was applied to precisely identify the worn regions on the CS surface. The dataset consisted of 909 preprocessed CS images, which were divided for training and testing purposes. The results indicated that the proposed CNN model achieved a prediction accuracy of 70.14%, outperforming two widely used CNN architectures, ResNet50 (59.42%) and VGG16 (56.51%). These findings demonstrate that the proposed architecture is more suitable and effective for classifying and recognizing different wear patterns of CS. Zhou *et al.* (2024a) proposed a method combining CS anomaly detection based on the YOLOv8 model with computer vision techniques, together with classical algorithms for intelligent defect recognition, was proposed. The results showed that the algorithm achieved a recognition accuracy exceeding 90%, with an average processing time of 12.32 ms per image. The algorithm was found to perform effectively even under harsh environmental conditions.

Besides mechanical wear caused by friction, another issue that has received considerable attention and severely affects the CS surface is electrical arcing. Electrical arcs can result in carbon strip erosion, damage to the CL, and interruption of power supply, while also generating interference in communication signals, which directly impacts train operation and poses a threat to operational safety.

Wei *et al.* (2025) developed a method for detecting electrical arcs was proposed based on a combination of machine learning, current signals, and electromagnetic radiation. First, arc data were collected using a pantograph–contact line arc simulation platform integrated with custom sensors. Next, the Ensemble Empirical Mode Decomposition (EMD) method was applied to decompose both the current and electromagnetic radiation signals. Subsequently, key features highly correlated with the arc state were selected through a rolling time-window combined with an improved F-score algorithm, significantly reducing feature redundancy and enhancing model robustness. Then, three different optimization algorithms were compared for application to the Support Vector Machine (SVM) model, with the Grey Wolf Optimizer (GWO) combined with SVM being identified as optimal. Finally, the dual-information approach – Ensemble EMD – improved F-score – GWO – SVM achieved an accuracy of 97.65% and an error of 2.53% in detecting electrical arcs. An experimental dataset based on the pantograph–contact line platform was established in combination with a finite element method (FEM) model built on magnetohydrodynamics (MHD). Meanwhile, arc erosion images were captured using an electron microscope to analyze the arc discharge phenomenon (Pan *et al.*, 2025). The results indicated that during pantograph raising, the reduction of the gap and narrowing of the arc column caused the heat flux to concentrate strongly at the contact point, resulting in a maximum temperature of 3550 K on the CL and 4290 K on the CS, forming a “deep and narrow” molten pool with a depth more than 80% greater than that observed during lowering, increasing the risk of material damage due to thermal and stress concentration. Conversely, during pantograph lowering, the increased gap led to a more dispersed heat flux and reduced temperature, forming a “shallow and wide” molten pool with weaker evaporation but more pronounced spattering, which accelerated material wear. Marangoni effects and vortices within the molten pool facilitated more uniform heat distribution but also caused surface instabilities, further exacerbating damage. In addition, the arc discharge velocity significantly influenced the molten pool morphology, with higher velocities causing pool contraction and reduced heat flux density. Yang *et al.* (2024a) established electromagnetic interference caused by arc discharge under high voltage and current conditions was investigated, as illustrated in Figure 10. The results indicated that the electric field spectrum exhibited radiated interference in the range of 30–125 MHz, with amplitudes varying from 60 dBμV/m to 123 dBμV/m. When the supply voltage increased from 20% of Umax to 80% of Umax, the radiation intensity at 125 MHz was observed to increase by approximately 10 dB.

5. Open issues and future research directions

Despite significant advances in understanding the wear mechanisms and material optimization of pantograph contact strips, several challenges remain that require further investigation. First,

Figure 10. Arc phenomenon between the CL and pantograph. **Source(s):** Yang *et al.* (2024b)

the complex interplay between mechanical, electrical, and thermo-mechanical factors under high-speed operation is not yet fully quantified. Existing wear models, while capable of capturing individual mechanisms such as adhesive, abrasive, and fatigue wear, often fail to predict coupled electro-mechanical degradation under variable environmental and operational conditions. Future studies should focus on developing multi-physics models that integrate mechanical contact, arc-induced thermal effects, and dynamic pantograph behavior to accurately simulate real-world wear patterns.

Second, although material innovations such as metal-impregnated carbon and fiber-reinforced composites have demonstrated improved wear resistance, conductivity, and impact tolerance, their long-term performance under fluctuating current loads and extreme environmental conditions remains underexplored. The effects of high humidity, salt-laden atmospheres, temperature cycling, and airborne particulates on composite microstructure, metal impregnation stability, and arc erosion require systematic experimental validation. Research into novel hybrid materials with self-lubricating and arc-resistant properties could further enhance the durability of contact strips.

Third, the monitoring and predictive maintenance of pantograph systems remain constrained by limitations in sensing technologies and data analytics. While optical scanning, 3D imaging, and machine learning-based approaches have enabled more accurate and automated wear detection, the real-time prediction of imminent failures is still challenging, particularly under high-speed and high-current operating conditions. Future work should integrate high-resolution sensor data, advanced computer vision, and deep learning frameworks for real-time, predictive assessment of contact strip health. In addition, the fusion of electrical, thermal, and mechanical signals may improve the reliability of fault detection algorithms, especially for detecting arc erosion and early-stage micro-cracking.

Finally, the influence of pantograph design, catenary geometry, and operational control strategies on wear evolution is not fully exploited. Optimizing pantograph stiffness, damping, and contact force regulation in conjunction with real-time environmental feedback could mitigate both mechanical and electro-mechanical wear. Moreover, the development of adaptive catenary systems or self-optimizing pantographs may allow the dynamic distribution of contact stress, reducing localized degradation and extending component lifetime.

Future research should adopt an integrated approach combining material science, tribology, electromagnetism, environmental effects, and intelligent monitoring. Such efforts will facilitate the design of more durable, reliable, and high-performance PCS, meeting the demands of next-generation high-speed rail networks.

6. Conclusion

With the increasing operating speeds of trains, issues such as unstable contact between the pantograph and the CL, wire oscillations, and abnormal wear have become more prominent, leading to poorer current quality. Therefore, research on electric-current-induced wear in pantograph systems has emerged as a critical direction to clarify wear mechanisms, progression patterns, and to improve contact quality while reducing abnormal wear. This research holds significant technical importance, contributing to enhanced operational safety and reduced maintenance costs. The CS and CL form a typical wear pair influenced by multiple factors, including pantograph parameters, train speed, operating environment, structure, and material. Wear of the CS can be classified by mechanism into mechanical wear, electrical wear, and electro-mechanical wear, with each mechanism contributing differently depending on operating conditions. The CS materials have evolved from pure metals, pure carbon, powder metallurgy, and metal-impregnated carbon to advanced composites. Among these, carbon/carbon composites stand out due to their wear resistance, thermal stability, and industrial manufacturing potential. In the future, the development of new materials aligned with sustainable practices and the utilization of available resources is expected to enhance self-lubrication, resistance to wear and arcing, as well as current collection efficiency and dynamic stability. Research and optimization of CS materials, combined with CL system design, represent a key direction to ensure efficient power transmission, extended service life, and operational safety for future electrified high-speed train systems.

References

Abd Majid, N., & Mohd Zaki, N. (2025). A systematic review of transportation rail networks: Impacts on urban development and sustainability. *International Journal of Academic Research in Business and Social Sciences*, *15*(2), 236–256. doi: 10.6007/ijarbss/v15-i2/24438.

Agarwal, N., Rangamani, A., Bhavsar, K., Virnodkar, S. S., Agostinho, A., Chadha, U., . . . Rajasekharan, V. (2024). An overview of carbon-carbon composite materials and their applications. *Frontiers in Materials*, *11*, 1374034. doi: 10.3389/fmats.2024.1374034.

Amano, Y., Kobayashi, S., Yabuno, H., Yamashita, Y., & Mori, H. (2024). Mechanism and suppression of friction-induced vibration in catenary-pantograph system. *Nonlinear Dynamics*, *112*(17), 14959–14980. doi: 10.1007/s11071-024-09802-6.

Ansari, M. S., Zafar, S., & Pathak, H. (2023). A comprehensive review of surface modification techniques for carbon fibers for enhanced performance of resulting composites. *Results in Surfaces and Interfaces*, *12*, 100141. doi: 10.1016/j.rsurfi.2023.100141.

Archard, J. F. (1953). Contact and rubbing of flat surfaces. *Journal of Applied Physics*, *24*(8), 981–988. doi: 10.1063/1.1721448.

Atazadeh, N., Heydari, M. S., Baharvandi, H. R., & Ehsani, N. (2016). Reviewing the effects of different additives on the synthesis of the Ti_3SiC_2 MAX phase by mechanical alloying technique. *International Journal of Refractory Metals & Hard Materials*, *61*, 67–78.

Ban, J., Zhou, C., Feng, L., Jia, Q., Liu, X., & Hu, J. (2020). Preparation and application of ZrB_2-SiCw composite powder for corrosion resistance improvement in Al_2O_3–ZrO_2–C slide plate materials. *Ceramics International*, *46*(7), 9817–9825. doi: 10.1016/j.ceramint.2019.12.255.

Biswas, P., Nayak, J., Kundu, A., Patel, D., Mallik, A., & Das, S. (2024). A review on the development of processing techniques for the production and casting of Al-alloy and metal matrix composite material. *Iranian Journal of Science and Technology, Transactions of Mechanical Engineering*, *49*(1), 35–66. doi: 10.1007/s40997-024-00773-y.

Bruni, S., Bucca, G., Facchinetti, A., Gregori, S., & Pombo, J. (2025). Recent developments on pantograph-overhead line interaction. *Vehicle System Dynamics*, *63*(7), 1358–1394. doi: 10.1080/00423114.2025.2484453.

Cantürk, S. B., & Kováčik, J. (2022). Review of recent development in copper/carbon composites prepared by infiltration technique. *Energies*, *15*(14), 5227. doi: 10.3390/en15145227.

Daneshian, B., Höche, D., Knudsen, O. Ø., & Skilbred, A. W. B. (2023). Effect of climatic parameters on marine atmospheric corrosion: Correlation analysis of on-site sensors data. *npj Materials Degradation*, *7*(1), 1–10. doi: 10.1038/s41529-023-00329-6.

Daocharoenporn, S., & Mongkolwongrojn, M. (2023). Effects of crosswind on pantograph–catenary wear using nonlinear multibody system dynamic algorithms. *World Electric Vehicle Journal*, *14* (9), 250. doi: 10.3390/wevj14090250.

Derosa, S., Nåvik, P., Collina, A., Bucca, G., & Rønnquist, A. (2020). A heuristic wear model for the contact strip and contact wire in pantograph – catenary interaction for railway operations under 15 kV 16.67 Hz AC systems. *Wear*, *456-457*, 203401. doi: 10.1016/j.wear.2020.203401.

Derosa, S., Nåvik, P., Collina, A., Bucca, G., & Rønnquist, A. (2021). Contact point lateral speed effects on contact strip wear in pantograph – catenary interaction for railway operations under 15 kV 16.67 Hz AC systems. *Wear*, *486-487*, 204103. doi: 10.1016/j.wear.2021.204103.

Dong, K., Wu, G., Qian, P., Ma, Y., Yang, Z., Wei, W., & Gao, G. (2023). Research on motion characteristics of arc at low air pressure. In *2023 Panda Forum on Power and Energy (PandaFPE)* (pp. 1218–1222).

Dong, Y., Li, B., Chen, Z., Wang, H., & Zhang, H. (2025). A study on the pantograph slide wear model based on energy dissipation. *Applied Sciences*, *15*(12), 6748. doi: 10.3390/app15126748.

Du, W., Zhou, S., Yi, Z., Xiang, R., Liu, Y., Shi, Z., & Peng, S. (2025). Simulation analysis on fatigue damage mechanism and life assessment of rigid catenary pillar of railway lines. *Railway Sciences*, *4*(3), 337–355. doi: 10.1108/rs-01-2025-0001.

Fadzil, F. M., Hyie, K. M., & Selamat, M. A. (2023). Development and characterisation of pantograph slides for railway applications: A short review. *Jurnal Mekanikal*, *46*, 38–47. doi: 10.11113/jm.v46.486.

Haeg, S. (2025). High-performance pantograph testing, Available from: https://www.mts.com/en/articles/rail/high-performance-pantograph [accessed 3 January 2026].

Hayes, S., Fletcher, D. I., Beagles, A. E., & Chan, K. (2020). Effect of contact wire gradient on the dynamic performance of the catenary pantograph system. *Vehicle System Dynamics*, *59*(12), 1916–1939. doi: 10.1080/00423114.2020.1798473.

Hu, Y., Huang, P., Cheng, C., Zhang, M., & Ma, R. (2024). Influence of arc discharge on the temperature and wear behaviors of the contact strip in pantograph-rigid catenary systems under AC conditions. *Wear*, *546-547*, 205368. doi: 10.1016/j.wear.2024.205368.

Jia, C., Li, S., Guo, X., Su, J., & Song, K. (2023). Influence of service parameters on the current-carrying tribological properties of CF-Al_2O_3/Cu composites. *Industrial Lubrication and Tribology*, *75*(6), 706–713. doi: 10.1108/ilt-03-2023-0055.

Jiang, T., Wang, Y., Xiang, L., Tang, B., Shi, S., Jiang, C., . . . Yu, J. (2025). High-performance carbon/carbon composites with enhanced thermal conductivity via polyacrylonitrile fiber and pyrolytic carbon synergies. *Journal of Alloys and Compounds*, *1027*, 180620. doi: 10.1016/j.jallcom.2025.180620.

Karaduman, G., & Akin, E. (2020). A deep learning based method for detecting of wear on the current collector strips' surfaces of the pantograph in railways. *IEEE Access*, *8*, 183799–183812. doi: 10.1109/access.2020.3029555.

Kong, B., Ru, J., Zhang, H., & Fan, T. (2018). Enhanced wetting and properties of carbon/carbon-Cu composites with Cr_3C_2 coatings by Cr-solution immersion method. *Journal of Materials Science & Technology*, *34*(3), 458–465. doi: 10.1016/j.jmst.2017.01.028.

Kumar, P., & Srivastava, V. K. (2016). Tribological behaviour of C/C–SiC composites—a review. *Journal of Advanced Ceramics*, *5*(1), 1–12. doi: 10.1007/s40145-015-0171-z.

L. T graphite (2024). 32% Cu impregnated graphite scrubber applied on high speed train pantograph, Available from: https://lttrade.en.made-in-china.com/product/LKAJVNQxFupE/China-32-Cu-Impregnated-Graphite-Scrubber-Applied-on-High-Speed-Train-Pantograph.html [accessed 1 April 2026].

Lee, H., Kim, M., Kim, G., & Kim, D. (2023). Effect of the chemical properties of silane coupling agents on interfacial bonding strength with thermoplastics in the resizing of recycled carbon fibers. *Polymers*, *15*(21), 4273. doi: 10.3390/polym15214273.

Li, M., Ren, B., Wu, W., Jiang, K., Zhang, J., Xu, E., . . . Jiang, Y. (2022). Copper fiber reinforced needle-coke/carbon composite for pantograph slide and its current-carrying wear performance. *Materials Research Express*, *9*(5), 055605. doi: 10.1088/2053-1591/ac6ccd.

Li, B., Zhao, Y., Ji, R., Dong, H., & Wei, N. (2025). Arc dynamics and erosion behavior of pantograph-catenary contacts under controlled humidity levels. *Sensors*, *25*(16), 5208. doi: 10.3390/s25165208.

Liu, X., Yang, Z., Xiao, S., Duan, X., Gao, G., Wei, W., . . . Sykulski, J. K. (2020). Multi-physics analysis and optimisation of high-speed train pantograph–catenary systems allowing for velocity skin effect. *High Voltage*, *5*(6), 654–661. doi: 10.1049/hve.2019.0388.

Liu, X., Hu, M., Li, Z., Zhou, C., Xiao, Q., Yang, W., & Chen, D. (2021). Effect of copper contents on the current-carrying wear properties of carbon brush under different temperatures conditions. *Journal of Materials Research and Technology*, *15*, 3110–3121. doi: 10.1016/j.jmrt.2021.09.111.

Liu, Y., Mao, X., & Li, B. (2025). Study on the influence of salt spray environment on the friction and wear performance of bow net system and its optical characterization. In *Second International Conference on Electronics, Electrical, and Control System (EECS 2025)* (pp. 3).

Liu, K., Zhang, Z., Li, L., Zhao, L., & Zhou, Y. (2026). Research and application of diagnosis methods and devices for urban rail traction systems. *Railway Sciences*, *5*(1), 88–99. doi: 10.1108/rs-10-2025-0048.

Lu, S., Liu, Z., Li, D., & Shen, Y. (2021). Automatic wear measurement of pantograph slider based on multiview analysis. *IEEE Transactions on Industrial Informatics*, *17*(5), 3111–3121. doi: 10.1109/tii.2020.2997724.

Ma, Y., Wang, J., Zhao, Y., Wei, X., Ju, L., & Chen, Y. (2020). A new vacuum pressure infiltration CFRP method and preparation experimental study of composite. *Polymers*, *12*(2), 419. doi: 10.3390/polym12020419.

Mersen (2024). Current collection technical guide, Available from: https://www.mersen.com/sites/default/files/medias/files/2024-09/current-collection-technical-guide-mersen-EN-1601.pdf [accessed 10 December 2025].

Morgan advanced materials (2024). Performance carbon for traction current collectors, Available from: https://www.morganperformancecarbon.com/media/tjkmitgn/performance_carbon_traction_current_collector_2024_web_lr.pdf [accessed 10 December 2025].

Morteng (2024). Rail transit applications, Available from: https://www.morteng-group.com/uploads/Morteng-Catalogue-Railway1.pdf [accessed 1 April 2026].

Nilson, P. (2023). Overhead lines vs third rail: How does rail electrification work?, Available from: https://www.railway-technology.com/features/overhead-lines-vs-third-rail-how-does-rail-electrification-work [accessed 2 July 2025].

Ning, Z., Xingshuai, Z., Jing, Z., Wei, Z., Chaoji, L., & Weihua, Z. (2024). Friction and wear performance of pantograph-catenary system in electrified railways: State of the art. *Journal of Southwest Jiaotong University*, *59*(5), 990–1005.

Pan, L., Yi, X., Xing, T., Yu, Z., Yang, C., Yu, Q., . . . Yan, W. (2025). Arc erosion behaviors of pantograph of high-speed train during its rise and fall processes. *IEEE Access*, *13*, 165144–165156. doi: 10.1109/access.2025.3612260.

Pantrac (2024). High quality electrical contacts made of carbon, Available from: https://pantrac.de/wp-content/uploads/2024/06/PAN-PR-EN-US_2022-03-29-web2.pdf [accessed 10 December 2025].

Peng, X., Wu, Y., & Wei, Z. (2024). Research progress on the surface modification of carbon fiber. *RSC Advances*, *14*(6), 4043–4064. doi: 10.1039/d3ra08577e.

Permalu, S. V., & Nagarajoo, K. (2024). KL-SG High-Speed Rail – a catalyst for national economic development. *Railway Sciences*, *3*(3), 265–278. doi: 10.1108/rs-12-2023-0049.

Ren, W., & Chen, G. (2023). Experimental study on the wear mechanism of the contact line in rigid pantograph-catenary systems. *Tribology International*, *187*, 108739. doi: 10.1016/j.triboint.2023.108739.

Santamato, G., Chiaradia, D., Solazzi, M., & Frisoli, A. (2023). Detecting early damages in the railway pantograph mechanism: A multiple excitation approach for the frequency domain. *Vehicle System Dynamics*, *62*(6), 1495–1516. doi: 10.1080/00423114.2023.2242529.

Simarro, M., Postigo, S., Casanueva, C., Rodríguez-Tembleque, L., & Castillo, J. J. (2024). Influence of main operating conditions on contact wire wear of rigid catenary lines. *Tribology International*, *196*, 109708. doi: 10.1016/j.triboint.2024.109708.

Song, C., Sun, Y., Zhang, Y., Pang, X., Chen, T., Sun, C., & Zhang, Y. (2021). Current-carrying property and damage mechanism of rolling contact pairs in different water conditions: From vapor to liquid. *Wear*, *477*, 203857. doi: 10.1016/j.wear.2021.203857.

Song, Y., Mei, G., Liu, Z., & Gao, S. (2023). Assessment of railway pantograph-catenary interaction performance with realistic pantograph strip imperfection. *Vehicle System Dynamics*, *62*(9), 2355–2374. doi: 10.1080/00423114.2023.2289662.

Song, E., Bi, Y., & Wu, A. (2025). Multi-field modelling and temperature rise analysis for the pantograph-catenary contact of metro train during a temporary stop. *Proceedings of the Institution of Mechanical Engineers, Part C: Journal of Mechanical Engineering Science*, *2*, 09544062241312565. doi:10.1177/09544062241312565.

Sunar, Ö., & Fletcher, D. (2023). Experimental investigation on the arc damage and fatigue crack initiation risk of copper-silver contact wires. *IEEE Transactions on Power Delivery*, *38*(2), 777–784. doi: 10.1109/tpwrd.2022.3198734.

Tan, H., Wang, Y., Wang, C., Wang, C., Li, M., Jiang, H., & Xu, Z. (2022). Laminate design of carbon-fiber-reinforced resin matrix composites for optimized mechanical properties and electrical conductivity. *Materials*, *15*(22), 7876. doi: 10.3390/ma15227876.

Tian, R., Wang, S.-J., Lu, M., & Li, J. (2025). Study on the ablation of slide plate by pantograph–catenary arc based on pantograph slide material. *Infrastructures*, *10*(10), 276. doi: 10.3390/infrastructures10100276.

Tian, Y., Li, W., Wang, H., Ma, Y., Li, C., & Sheng, X. (2026). Enhancing corrosion and wear resistance of phosphate coatings using fly ash as an accelerating agent. *Colloids and Surfaces A: Physicochemical and Engineering Aspects*, *728*, 138661. doi: 10.1016/j.colsurfa.2025.138661.

Wang, W., Liang, Y., Zhang, W., & Iwnicki, S. (2019). Experimental research into the low-temperature characteristics of a hydraulic damper and the effect on the dynamics of the pantograph of a high-speed train running in extreme cold weather conditions. *Proceedings of the Institution of Mechanical Engineers, Part F: Journal of Rail and Rapid Transit*, *234*(8), 896–907. doi: 10.1177/0954409719879029.

Wang, P., Wang, L., Kang, K., Yin, J., Xiong, X., & Zhang, H. (2020). Microstructural, mechanical and tribological performances of carbon fiber reinforced copper/carbon composites. *Composites Part A: Applied Science and Manufacturing*, *142*, 106247. doi: 10.1016/j.compositesa.2020.106247.

Wang, P., Jia, Y., Li, Y., Liu, Y., Hao, Z., Deng, G., & Wang, L. (2021). Microstructural, mechanical and tribological performances of copper foam modified CFRP composite for pantograph strip. *Journal of Applied Polymer Science*, *138*(36), 50901. doi: 10.1002/app.50901.

Wang, H., Gao, G., Wei, W., Yang, Z., Yin, G., Xie, W., . . . Wu, G. (2022a). Influence of the interface temperature on the damage morphology and material transfer of C–Cu sliding contact under different current amplitudes. *Journal of Materials Science*, *57*(8), 5006–5021. doi: 10.1007/s10853-022-06935-0.

Wang, Z., Su, K., Gao, J., Jia, Q., Zhang, Z., & Liu, X. (2022b). Preparation, microstructure and properties of Al2O3–ZrO2–C slide plate material in presence of nanoscale oxides. *Ceramics International*, *48*(7), 10126–10135. doi: 10.1016/j.ceramint.2021.12.223.

Wang, P., Xie, F., Wexler, D., Yin, J., Zhang, H., & Zhu, H. (2023). Tribological behaviors of copper modified carbon/carbon composites for pantograph strip under electric current conditions. *Tribology International*, *185*, 108483. doi: 10.1016/j.triboint.2023.108483.

Wang, P., Wang, S., Ge, J., Si, D., & Yang, D. (2023b). Study on wear characteristics and authorized limits of switch rails of high-speed turnout. *Railway Sciences*, *2*(2), 157–169. doi: 10.1108/rs-03-2023-0014.

Wei, W., Zeng, K., Wan, Y., Xia, L., Zhang, H., & Yang, Z. (2025). A pantograph-catenary arcing detection method based on the fusion of current and electromagnetic radiation. *Engineering Research Express*, *7*(3), 035346. doi: 10.1088/2631-8695/adf9c0.

Wu, G., Dong, K., Xu, Z., Xiao, S., Wei, W., Chen, H., . . . Huang, X. (2022a). Pantograph–catenary electrical contact system of high-speed railways: Recent progress, challenges, and outlooks. *Railway Engineering Science*, *30*(4), 437–467. doi: 10.1007/s40534-022-00281-2.

Wu, Q., Gu, X. P., Ma, Z., & Wang, A. (2022b). A study on the vibration characteristics and damage mechanism of pantograph strips in a railway electrification system. *Machines*, *10*(8), 710. doi: 10.3390/machines10080710.

Wu, R., Song, C., Wu, H., Lv, B., Zhang, Y., & Zhang, Y. (2022c). Effect of relative humidity on the current-carrying tribological properties of Cu–C sliding contact pairs. *Wear*, 492–493, 204219, doi 10.1016/j.wear.2021.204219

Xu, Z., Gao, G., Wei, W., Yang, Z., Xie, W., Dong, K., . . . Wu, G. (2021). Characteristics of pantograph-catenary arc under low air pressure and strong airflow. *High Voltage*, *7*(2), 369–381. doi: 10.1049/hve2.12180.

Xu, Y., Liu, Z. D., Stichel, S., Zhu, W. D., Lei, J. L., & Yao, Y. (2024). A comparative study on the influence of typical track failures on high-speed pantograph-catenary interaction dynamics. *Vehicle System Dynamics*, *62*(11), 2883–2911. doi: 10.1080/00423114.2024.2305295.

Yang, L., Wang, Y., Lian, Y., Dong, X., Liu, J., Liu, Y., & Wu, Z. (2022). Rational planning strategies of urban structure, metro, and car use for reducing transport carbon dioxide emissions in developing cities. *Environment, Development and Sustainability*, *25*(7), 6987–7010. doi: 10.1007/s10668-022-02344-0.

Yang, Y., Cao, H., Zhang, M., Su, Z., Hu, M., Jin, M., & Liu, S. (2024a). Research on the influence of pantograph catenary contact loss arcs and zero-crossing stage on electromagnetic disturbance in high-speed railway. *Energies*, *17*(1), 138. doi: 10.3390/en17010138.

Yang, K., Liu, Y., Li, X., Bai, Z., Wan, Y., Xiao, Y., & Li, J. (2024b). A high-accuracy single-frame 3D reconstruction method with color speckle projection for pantograph sliders. *Measurement*, *237*, 115192. doi: 10.1016/j.measurement.2024.115192.

Yao, Y., Zhou, N., Mei, G., & Zhang, W. (2020). Dynamic analysis of pantograph-catenary system considering ice coating. *Shock and Vibration*, *2020*, 1–15. doi: 10.1155/2020/8887609.

Yao, X., Xing, Z., Sheng, A., & Chen, Y. (2022). An image-based online monitoring system for pantograph wear and attitude. *IEEE Transactions on Instrumentation and Measurement*, *71*, 5013812, 1–12. doi:10.1109/TIM.2022.3178466.

Zhang, K. X., Guo, X. S., Zhao, W. K., Zhang, F. Q., & He, L. L. (2020). TEM study on the microstructure of the interface at the scale of nanometer formed between Cu-8 wt.% Ti melt and C/C preform. *Materials Chemistry and Physics*, *246*, 122795. doi: 10.1016/j.matchemphys.2020.122795.

Zhang, H., Goltsberg, R., & Etsion, I. (2022). Modeling adhesive wear in asperity and rough surface contacts: A review. *Materials*, *15*(19), 6855. doi: 10.3390/ma15196855.

Zhao, F., Liu, J., Zhang, C., Zhao, Z., Ning, X., & Wang, J. (2025). Current development and prospect of national science and technology innovation platform in the railway industry. *Railway Sciences*, *4*(2), 266–279. doi: 10.1108/rs-12-2024-0055.

Zhi, X., Zhou, N., Wei, H., Chen, H., Cheng, Y., Sun, Y., . . . Zhang, W. (2025). Analysis of the abnormal wear of the pantograph contact strip through combined experimental and simulation approaches. *Scientific Reports*, *15*(1), 45706. doi: 10.1038/s41598-025-28380-0.

Zhi, X., Zhou, N., Cheng, Y., Wei, H., Yao, Y., Zhang, W., & Chen, G. (2026). Study on wear performance and mechanism of pantograph contact strip that contact with damaged contact wire under ambient humidity. *Friction*, *14*(2), 9441101. doi: 10.26599/frict.2025.9441101.

Zhou, R., Xiang, B., Wu, L., Hu, Y., Dou, L., & Huang, K. (2024a). Research on intelligent identification method of pantograph positioning and skateboard structural anomalies based on improved YOLO v8 algorithm. In *Transportation Science and Technology.*

Zhou, N., Zhi, X., Cheng, Y., Sun, Y., Wang, J., Gu, Z., . . . Zhang, W. (2024b). Contact strip of pantograph heuristic wear model and its application. *Tribology International*, *194*, 109546. doi: 10.1016/j.triboint.2024.109546.

Zuo, H., Wei, W., Yang, Z., Li, X., Xie, W., Liao, Q., . . . Wu, G. (2021a). Synchronously improved mechanical strength and electrical conductivity of Carbon/Copper composites by forming Fe_3C interlayer at C/Cu interface. *Materials Today Communications*, *28*, 102661. doi: 10.1016/j.mtcomm.2021.102661.

Zuo, H., Wei, W., Yang, Z., Li, X., Ren, J., Xian, Y., . . . Wu, G. (2021b). Performance enhancement of carbon/copper composites based on boron doping. *Journal of Alloys and Compounds*, *876*, 160213. doi: 10.1016/j.jallcom.2021.160213.

Zuo, H., Wei, W., Li, X., Yang, Z., Liao, Q., Xian, Y., & Wu, G. (2021c). Enhanced wetting and properties of Carbon/Copper composites by Cu-Fe alloying. *Composite Interfaces*, *29*(1), 111–120. doi: 10.1080/09276440.2021.1904720.

Corresponding author
Dong Doan Van can be contacted at: dongdv@ut.edu.vn

Dong Doan Van serves as Vice Dean of the Institute of Mechanical Engineering at UTH and Head of the Big Data Research for Infrastructure & Green Engineering (BRIDGE) Research Group. He received the Ph.D. degree from Wuhan University of Technology in 2018. He served as Dean of the Faculty of Electrical and Electronics Engineering at UTH in 2019 and as Head of the Training Department in 2022. His research interests include railway transportation systems, the Vehicular Internet of Things (VIoT), intelligent transportation systems, energy efficiency, and control systems in transportation. He has published more than 50 conference papers, book chapters, and journal articles.